

Silver-Guided Excimer Emission in an Adenine–Pyrene Conjugate: Fluorescence Lifetime and Crystal Studies

Mrituanjay D. Pandey, Ashutosh Kumar Mishra, Vadapalli Chandrasekhar,* and Sandeep Verma*

Department of Chemistry, Indian Institute of Technology Kanpur, Kanpur 208016, India

Received November 6, 2009

This Communication describes a novel adenine–pyrene conjugate (**1**) and its solid-state structure with silver and copper ions. Single-crystal studies of metal complexes of **1** offer insight into molecular interactions and provide a basis to rationalize possible interactions in the solution state, leading to excimer formation. The robust nature of this interaction was further confirmed by deposition of the silver complex on a graphite surface, which exhibited a remarkable resemblance to its solid-state structure. The structural basis of selective excimer formation in the presence of Ag⁺ ions presents a viable approach for ratiometric detection of these ions.

The use of silver in the photographic, imaging, and electronics industries inadvertently results in increased silver bioaccumulation, leading to enhanced exposure and adverse biological effects and toxicity in aquatic and terrestrial organisms.¹ Silver ions are known to interfere with biochemical processes by enzyme/protein inactivation and ionoregulatory imbalance.² Therefore, the design and development of sensitive and selective methods for the determination of trace

quantities of silver ions is relevant to the environment and human health. Techniques such as atomic absorption spectroscopy, inductively coupled plasma mass spectroscopy, and potentiometry have been employed for silver ion detection.³ Recent reports have described fluorescence-based ratiometric measurement approaches to achieve better selectivity over conventional techniques.⁴

Herein, we report the synthesis and structural characterization of a novel adenine–pyrene conjugate, selective sensing of silver ions via excimer formation, and crystallographic investigations explaining the specific detection of silver ion over copper, another coinage metal.

Our group has dealt with silver–adenine coordination, leading to the formation of interesting and diverse supramolecular architectures.⁵ The facile formation of silver–adenine complexes and their luminescent properties led us to design a modified purine nucleobase that can not only coordinate with silver ions but also exhibit augmented luminescence due to an attached pyrene pendant group.

With this intention, we prepared a pyrene-based adenine analogue, 9-[2-[(pyren-1-ylmethyl)amino]ethyl]-9H-purin-6-amine (**1**; Scheme 1), and investigated its fluorescence behavior in the presence of various metal ions. Screening of **1**, in the presence of metal perchlorates, revealed a high selectivity for silver over other metal ions (Figure 1a). As shown in Figure 1a, the I_{470}/I_{375} ratio for silver was very high compared to other metal ions, with the lowest being that for the copper ions.

The emission spectra of **1**, when excited at 326 nm, show vibronic bands with peaks at around 375 and 397 nm, which could be attributed to pyrene emission. A significant decrease in vibronic emission was observed with simultaneous enhancement at 470 nm, when **1** was titrated with silver perchlorate because of the formation of a pyrene excimer (Figure 1b). Fluorescence lifetime measurements monitored at the excimer emission band, i.e., at 470 nm, exhibit longer decay times for the silver complex **2** (16.92 ns) compared to **1** alone (3.93 ns). This observation may be

*To whom correspondence should be addressed. E-mail: vc@iitk.ac.in (V.C.), sverma@iitk.ac.in (S.V.).

(1) (a) Webb, N. A.; Wood, C. M. *Aquatic Toxicol.* **2000**, *49*, 111–129. (b) Ratte, H. T. *Environ. Toxicol. Chem.* **1999**, *18*, 89–108. (c) Kazuyuki, M.; Nobuo, H.; Takatoshi, K.; Yuriko, K.; Osamu, H.; Yashihisa, I.; Kiyoko, S. *Clin. Chem.* **2001**, *47*, 763–766. (d) Purcell, T. W.; Peters, J. J. *Environ. Toxicol. Chem.* **1998**, *17*, 539–546.

(2) (a) Niemietz, C. M.; Tyerman, S. D. *FEBS Lett.* **2002**, *531*, 443–447. (b) Pedroso, M. S.; Bersano, J. G.; Bianchini, A. *Environ. Toxicol. Chem.* **2007**, *26*, 2158–2165. (c) Wells, T. N. C.; Scully, P.; Paravicini, G.; Proudfoot, A. E. I.; Payton, M. A. *Biochemistry* **1995**, *34*, 7896–7903.

(3) (a) Pu, Q. S.; Sun, Q. Y.; Hu, Z. D.; Su, Z. X. *Analyst* **1998**, *123*, 239–243. (b) Kimura, K.; Yajima, S.; Tatsumi, K.; Yokoyama, M.; Oue, M. *Anal. Chem.* **2000**, *72*, 5290–5294. (c) Ceresa, A.; Radu, A.; Peper, S.; Bakker, E.; Pretsch, E. *Anal. Chem.* **2002**, *74*, 4027–4036. (d) Mazloum, M.; Niassary, M. S.; Chahooki, S. H. M.; Amini, M. K. *Electroanalysis* **2002**, *14*, 376–380. (e) Chung, S.; Kim, W.; Park, S. B.; Yoon, I.; Lee, S. S.; Sung, D. D. *Chem. Commun.* **1997**, 965–966. (f) Teixidor, F.; Flores, M. A.; Escriche, L.; Vinas, C.; Casabo, J. *Chem. Commun.* **1994**, 963–964.

(4) (a) Yu, C.; Yam, W.-W. *Chem. Commun.* **2009**, 1347–1349. (b) Xu, Z.; Singh, J. N.; Lim, J.; Pan, J.; Kim, H. N.; Park, S.; Kim, K. S.; Yoon, J. *J. Am. Chem. Soc.* **2009**, *131*, 15528–15533. (c) Zhang, R.; Tang, D.; Lu, P.; Yang, X.; Liao, D.; Zhang, Y.; Zhang, M.; Yu, C.; Yam, V. W. W. *Org. Lett.* **2009**, *11*, 4302–4305. (d) Liu, L.; Zhang, D.; Zhang, G.; Xiang, J.; Zhu, D. *Org. Lett.* **2008**, *10*, 2271–2274 and references cited therein. (e) Lee, H. N.; Singh, N. J.; Kim, S. K.; Kwon, J. Y.; Kim, Y. Y.; Kim, K. S.; Yoon, J. *Tetrahedron Lett.* **2007**, *48*, 169–172.

(5) (a) Purohit, C. S.; Verma, S. *J. Am. Chem. Soc.* **2006**, *128*, 400–401. (b) Purohit, C. S.; Mishra, A. K.; Verma, S. *Inorg. Chem.* **2007**, *46*, 8493. (c) Purohit, C. S.; Verma, S. *J. Am. Chem. Soc.* **2007**, *129*, 3488–3489. (d) Kumar, J.; Verma, S. *Inorg. Chem.* **2009**, *48*, 6350–6352. (e) Mishra, A. K.; Purohit, C. S.; Verma, S. *CrystEngComm* **2008**, *10*, 1296–1298. (f) Verma, S.; Mishra, A. K.; Kumar, J. *Acc. Chem. Res.* **2010**, *43*, 79–91.

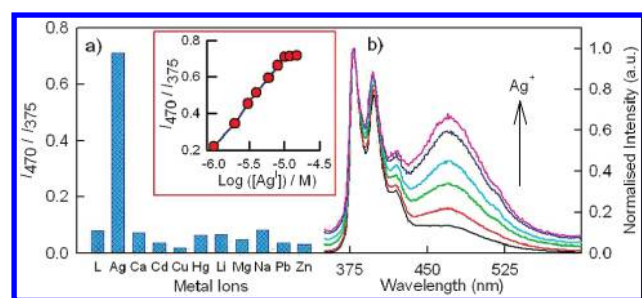
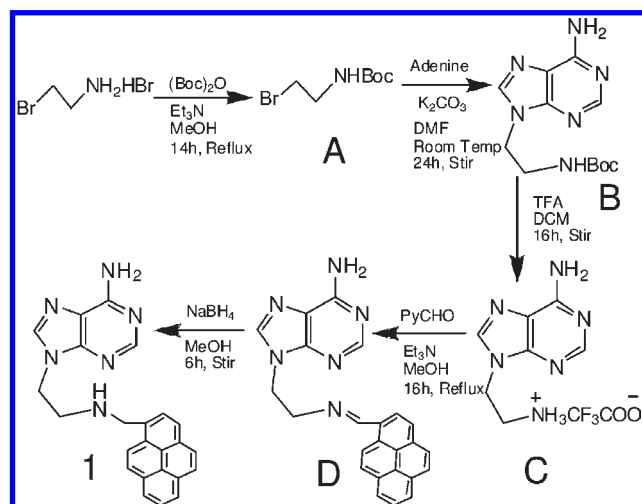
Scheme 1. Synthetic Scheme for **1**

Figure 1. (a) Ratio of excimer and monomer emission of **1** at 470 and 375 nm (I_{470}/I_{375} ; $1 \mu\text{M}$ in aqueous acetonitrile; 1:1, v/v) in the presence of various metal ions. (b) Fluorescence spectra of **1** with an increasing concentration of Ag^+ ions ($\lambda_{\text{exc}} = 326 \text{ nm}$). Color code: black, $0 \mu\text{M}$; red, $1 \mu\text{M}$; green, $2 \mu\text{M}$; cyan, $4 \mu\text{M}$; blue, $8 \mu\text{M}$; pink, $10 \mu\text{M}$. Inset: Plot of fluorescence ratios (I_{470}/I_{375}) of **1** vs $\log [\text{Ag}^+]/M$.

ascribed to a stable intermolecular pyrene excimer formation in solution (Figure 2a).⁶ A red shift of $\sim 20 \text{ nm}$ was observed in the excitation spectra of **2** during monitoring at the monomer (375 nm) and excimer (470 nm) regions, suggesting the occurrence of a static pyrene excimer (Figure 2b). We also observed that the excimer behavior of **1** in the solid state is similar to that of **2** in the solution state, while solid-state fluorescence of **2** showed a more prominent and red-shifted excimer emission.⁶ The concentration-dependent emission spectral studies suggest that the exciplex formation between adenine and pyrene moieties cannot be completely ruled out.⁶

We decided to determine the solid-state structures of silver and copper complexes of **1** to obtain insight into the organization of the ligand in the presence of metal ions. The asymmetric unit of **2**, $[(\text{C}_{24}\text{H}_{20}\text{AgN}_6)(\text{NO}_3)]_n$, consisted of one silver ion neutralized by a nitrate anion and simultaneously coordinated to three different nitrogens: N3 and N7 from two different adenine moieties and a side-chain nitrogen atom. This arrangement leads to a distorted trigonal-pyramidal geometry around the silver ion (Figure 3). A closer inspection of complex **2**, when viewed along the c axis, revealed that two adenine moieties from two ligands are connected by intervening silver ions via an unusual N3 and

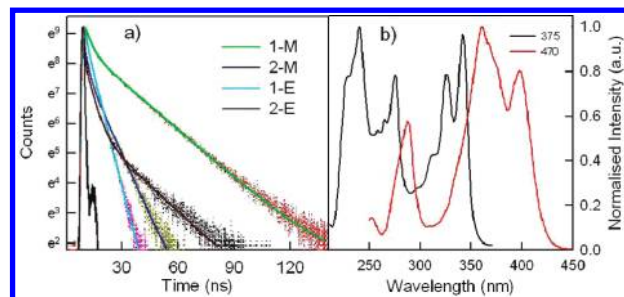


Figure 2. (a) Emission decays of the monomers (M), $\lambda_{\text{em}} = 375 \text{ nm}$, and excimers (E), $\lambda_{\text{em}} = 470 \text{ nm}$, of **1** and **2** in aqueous acetonitrile ($1 \mu\text{M}$; 1:1, v/v). (b) Excitation spectra of **2** at 375 and 470 nm.

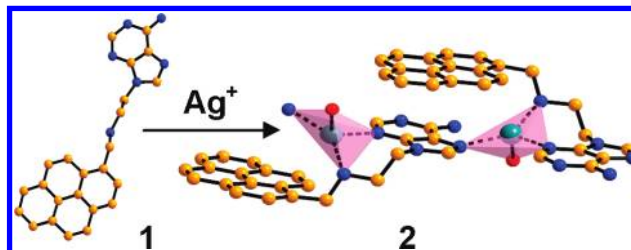


Figure 3. Representation of the silver complex **2**: formation of a 1D polymeric chain where the adjacent adenine-pyrene conjugates are tethered via a silver ion. Hydrogen atoms, solvent molecules, and counterions are omitted for clarity.

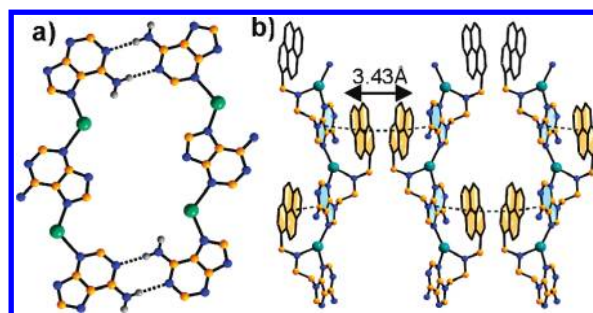


Figure 4. (a) Hydrogen-bonding interactions between the two polymeric chains in **2** resulting in the formation of virtual boxlike arrangement. Part of the ligand is omitted for clarity. (b) View of the crystal lattice of **2** along the c axis, showing a 1D coordination polymer, interconnected via stacked pyrene rings.

N7 coordination, thereby bringing pyrene moieties of two such ligands in close proximity in the solid state.

A significant feature of **2** is the interconnection of two 1D polymeric chains through hydrogen-bonding interactions occurring via the Watson-Crick face (i.e., N1 and N6-H) of adjacent adenine moieties, giving rise to the formation of a virtual rectangular box involving four silver ions and six adenine moieties (Figure 4a). The stability of this molecular box is reinforced by in-space hydrogen-bonding interactions between oxygen atoms of the nitrate group with C8-H and N6 hydrogen atoms.⁶ Notably, the intermolecular π - π interactions between the adenine moiety and the pyrene ring, where one adenine moiety is π - π -stacked from the top and another adjacent one from the bottom of a pyrene-pyrene stack, provide further stability to the crystal lattice (Figure 4b).

2, when viewed along the a axis, reveals two coordination polymeric chains running antiparallel to each other. This orientation of the polymeric chains is defined when one

(6) See the Supporting Information for details.

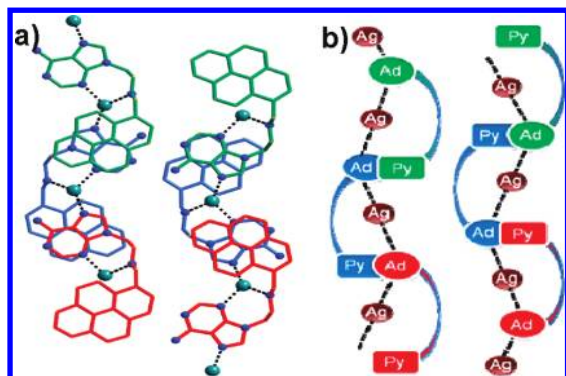


Figure 5. (a) Representation of the crystal lattice through *a*-axis showing antiparallel arrangement of polymeric chain with respect to adenine pyrene units. (b) Pictorial representation of an antiparallel arrangement of the polymeric chains.

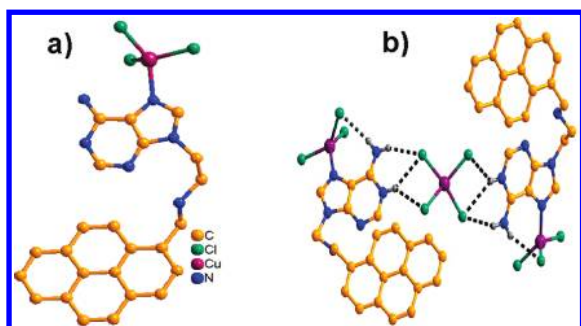


Figure 6. (a) Discrete unit of **3** showing copper coordination through the N7 atom of the adenine moiety. (b) Crystal lattice of **3** depicting the presence of two crystallographically unique copper ions and hydrogen-bonding interaction.

“adenine–pyrene” polymeric motif and a “pyrene–adenine” motif run opposite to one another (Figure 5).

Copper complex **3**, [(C₂₄H₂₂Cl₃CuN₆)₂(CuCl₄)], exhibits coordination only via the N7 atom, resulting in a discrete monomeric unit (Figure 6a). An interesting aspect of the crystal structure of **3** is the presence of two crystallographically unique copper ions: one as [CuCl₃][−] directly coordinated with an adenine moiety and the other as [CuCl₄]^{2−} in the crystal lattice (Figure 6b).⁷ The [CuCl₄]^{2−} species participates via in-space hydrogen-bonding interaction with the adjacent adenine moiety through N6–H and protonated N1–H, thus connecting two monomeric units. The formation of discrete monomeric units in the solid state perhaps explains the inability of copper to be detected by **1** via excimer formation in the solution state.

Supported by literature reports and our own investigations concerning patterning of coordination complexes on surfaces, we envisaged deposition of **2** on the graphite surface to assess the solution-state stability of this complex.^{5,8} The aggregative propensity of **2**, via silver coordination, was

(7) Bontchev, P. R.; Ivanova, B. B.; Bontchev, R. P.; Mehandjiev, D. R. *Polyhedron* **2001**, *20*, 231–236.

(8) (a) Ruben, M.; Lehn, J. M.; Muller, P. *Chem. Soc. Rev.* **2006**, *35*, 1056–1067 and references cited therein. (b) Barth, J. V.; Costantini, G.; Kern, K. *Nature* **2005**, *437*, 671–679.

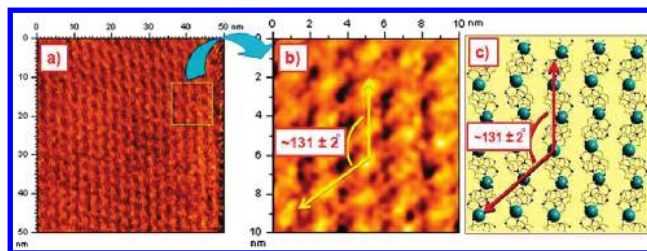


Figure 7. (a) AFM micrograph of **2** with repetitively patterned surfaces on HOPG. (b) Magnified image showing a diagonal angle between the two layers. (c) Diagonal angle between the lines connecting silver atoms along the *a* axis in **2**.

probed by noncontact-mode atomic force microscopy (AFM) after deposition of a solution of **2** (10 μL, 0.1 μM) on freshly cleaved highly oriented pyrolytic graphite (HOPG) surface. Analysis of the AFM micrographs revealed the structured deposition of **2** (Figure 7a), and interestingly the gross morphological features in the micrograph could correspond to the crystal structure of **2**, viewed along the *a* axis. The cross-sectional angle between the two axes of the stripe-like pattern, as observed in the AFM micrograph, was found to be $131 \pm 2^\circ$ throughout the probed surface (Figure 7b). This angle was found to be nearly equal to the angle formed between the lines connecting the silver atoms in the crystal lattice along the *a* axis in two different directions (Figure 7c). Facile transfer of the solid-state architecture onto the surface suggests that some of the solid-state interactions and motifs are preserved in the solution state. In a control experiment, **1** or **3** does not give rise to an ordered ultrastructure on the surface.⁶

In conclusion, we have described the molecular structures of an adenine–pyrene conjugate (**1**), a silver–adenine–pyrene coordination polymer (**2**), and a copper–adenine–pyrene (**3**) complex. The data presented here imply that **1** can serve as a potential supramolecular sensor switch model for the detection of silver ion bioaccumulation, trafficking, and toxicity in living systems.⁹ The AFM micrograph pattern of **2** on the HOPG surface was remarkably similar to the crystal structure, suggesting the possibility of stable organized structural elements in **2** that remain intact in both the solid and solution states.

Acknowledgment. This work is supported by the Bio-inorganic Chemistry Initiative Project, DST, India (to V.C. and S.V.).

Supporting Information Available: Crystallographic data in CIF format, synthesis and characterization for **1–3**, crystallographic information and tables, fluorescence measurements, and AFM images. This material is available free of charge via the Internet at <http://pubs.acs.org>. CCDC numbers 752771–752774 contain the supplementary crystallographic data and can be obtained from the Cambridge Crystallographic Data Centre via www.ccdc.cam.ac.uk/data_request/cif.

(9) (a) Fabbrizzi, L.; Poggi, A. *Chem. Soc. Rev.* **1995**, *24*, 197–202. (b) Domaille, D. W.; Que, E. L.; Chang, C. J. *Nature Chem. Biol.* **2008**, *4*, 168–175. (c) McRae, R.; Bagchi, P.; Sumalekshmy, S.; Fahmi, C. J. *Chem. Rev.* **2009**, *109*, 4780–4827.